Missing-Link Macrocycles: Hybrid Heterocalixarene Analogues Formed from Several Different Building Blocks

Jonathan L. Sessler,*[a] Won-Seob Cho,[a] Vincent Lynch,[a] and Vladimír Král[b]

Abstract: The synthesis and structural characterization of hybrid heterocalix[4]arene analogues containing pyrrole, benzene, methoxy-substituted benzene, and pyridine subunits is described. Macrocycles **1** and **2**, examples of calix[2]benzene[2]pyrrole and calix[1]benzene[3]pyrrole systems, respectively, are synthesized by the condensation of pyrrole and an appropriate phenylbis(carbinol). Macrocycles **3** and **7**, examples of calix[2]benzene[1]pyridine[1]pyrrole and calix[1]pyridine[3]pyrrole, respectively, are synthesized by the use of a carbene-based pyrrole-to-pyridine ring-expansion procedure. Single-crystal X-ray analysis reveals that compounds **1a**, **1b**, and **2b** adopt 1,3-alternate conformations in the solid state, whereas compounds **3** and **7** display structures that are best described as "flattened partial cones" in terms of their conformation. (Series **a** refers to pure benzene-derived systems, whereas series **b** indicates macrocycles containing 5-methoxyphenyl subunits). In the solid state, the methoxy-functionalized macrocycles **1b** and **2b**, and the chloropyridine-containing macrocycle **7** exist as dimers. In the case of **1a** and **7**, these compounds interact with neutral solvent in the solid state. The conformations of the macrocycles in solution were explored by temperature-dependent proton NMR and NOESY spectral analysis. At 188 K, macrocycles **1a** and **2a** adopt flattened 1,3-alternate conformations, whereas macrocycles **3** and **7** exist in the form of flattened partial-cone conformations. Standard proton NMR titration analyses were carried out in the case of macrocycles **1a** and **2a**, and reveal that at least the second of these systems is capable of binding fluoride and chloride anions in CD_2Cl_2 solution at room temperature ($K_a = 571$ and $17\,M^{-1}$ in the case of **2a** and F^- and Cl^-, respectively).

Keywords: anion receptors · calixarenes · heterocycles · macrocycles

Introduction

Calixarenes, without a doubt, represent one of the most versatile and important of receptor systems currently being studied in the context of supramolecular chemistry; they have allowed for the construction of many elegant receptors for anions, cations, and neutral substrates and provide the building blocks needed to explore novel approaches to self-assembly and nanotechnology applications development.[1–3] The rich chemistry of the calixarenes is spawning efforts to generate new related systems with improved substrate binding properties or self-assembly characteristics. Most of this effort has been devoted to making modifications to the so-called upper and lower rims of the calixarene skeleton. However, recently attention has also begun to be focused on making more fundamental changes. One way this has been done is through the use of different (i.e., non-carbon) bridging elements, an approach that has led to, inter alia, the production of intriguing oxa-, aza-, and thiacalixarenes.[1–3] Another approach has involved the use of nonclassical building blocks, including heterocyclic species such as pyrrole,[4–6] thiophene,[7–11] indole,[12–19] furan,[9, 10, 20–24] and naphthalene.[25, 26] While some of the resulting, non-phenolic entities have been known for over a century, in most instances the relevant molecular recognition properties have only begun to be explored. For instance, the calix[4]pyrroles, a class of molecules first reported by Baeyer in 1886[27] have recently been found to display remarkable binding properties with anions and neutral substrates.[4, 28–32] This has led us to consider that further generalizations of the heterocalixarene theme could lead to the production of both new molecular entities and, possibly, novel receptors with unusual substrate-binding properties. Of particular interest here are hybrid systems that contain more than one kind of aromatic or heterocyclic building block.[33–38]

[a] Prof. Dr. J. L. Sessler, W.-S. Cho, Dr. V. Lynch
Department of Chemistry and Biochemistry
Institute for Cellular and Molecular Biology
The University of Texas at Austin
Austin, TX 78712-1167 (USA)
Fax: (+1) 512-471-7550
E-mail: sessler@mail.utexas.edu

[b] Prof. Dr. V. Král
Department of Analytical Chemistry
Institute of Chemical Technology
Technická 5, 166 28 Prague (Czech Republic)

Supporting information for this contribution is available on the WWW under http://www.wiley-vch.de/home/chemistry/ or from the author.

  0947-6539/02/0805-1134 $ 17.50+.50/0

Results and Disscussion

In a recent report,[39] we detailed a convenient one-step approach to the generation of mixed calix[*n*]pyrrole[*m*]pyridine systems ($n + m = 4$; $m \geq 2$) and wish to present here the synthesis of several new analogues, including prototypic-unsubstituted and 5-methoxy-functionalized *trans*-calix[2]-benzene[2]pyrrole, calix[1]benzene[3]pyrrole, and *trans*-calix[2]benzene[1]-3-chloropyridine[1]pyrrole macrocycles (**1**–**3**), which to the best of our knowledge represent unprecedented "missing links" within the generalized calixarene family of macrocycles.

The approaches used to prepare the mixed phenyl (series **a**) and methoxyphenyl-containing (series **b**) calix[2]benzene[2]-pyrrole and calix[1]benzene[3]pyrrole targets **1** and **2** are shown in Schemes 1 and 2, respectively. In the case of the more symmetric targets **1a** and **1b**, a direct condensation strategy was employed, wherein the 4-methoxy-substituted or unsubstituted phenylbis(carbinol) **4** is treated directly with pyrrole **5** under conditions of acid catalysis. After workup, involving washing with aqueous 1N NaOH solution and purification by column chromatography over silica gel, the hybrid macrocycles **1a** and **1b** were isolated in yields of 16 and 26%, respectively. Further treatment of the unsubstituted product **1a** with dichlorocarbene then produced the chloro-substituted calix[2]benzene[1]pyridine[1]pyrrole macrocycle **3** in 36% yield, a transformation that is also illustrated in Scheme 1.

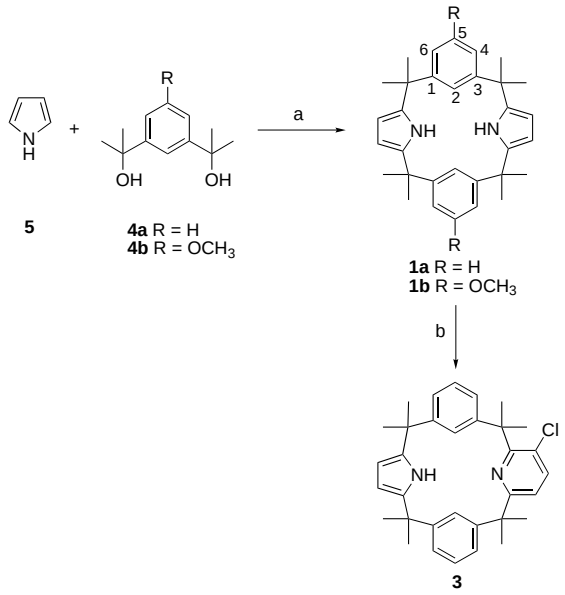

Scheme 1. Synthesis of macrocycles **1a**, **1b**, and **3**. a) $BF_3 \cdot Et_2O$, CH_3CN (**1a**: 16%, **1b**: 26%); b) dimethoxyethane, sodium trichloroacetate (36%).

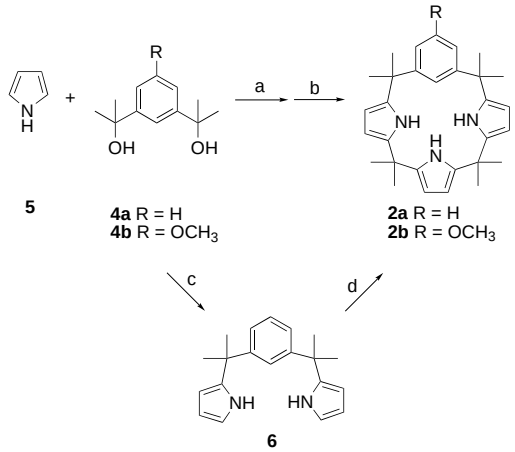

Scheme 2. Synthesis of macrocylces **2a** and **2b**. a) $BF_3 \cdot Et_2O$, CH_3CN, 5 min; b) acetone, 55 min (**2a**: 18%, **2b**: 13%); c) $BF_3 \cdot Et_2O$/excess pyrrole (68%); d) $BF_3 \cdot Et_2O$/acetone/pyrrole (**2a**: 20%).

In the case of the less symmetric hybrid calix[1]benzene[3]-pyrrole systems **2a** and **2b**, two strategies were tested. The first, analogous to that used to prepare **1**, involved simple $BF_3 \cdot Et_2O$-catalyzed treatment of the phenylbis(carbinol)s **4a** and **4b** with four equivalents of pyrrole **5** in the presence of acetone under an inert atmosphere. After quenching with triethylamine and purification over silica gel as in the case of **1a** and **1b**, macrocycles **2a** and **2b** were obtained in 18 and 13% yield, respectively.

In an effort to improve the yield of **2a**, the step-wise procedure summarized in Scheme 2 was attempted. In this case, the $BF_3 \cdot Et_2O$-catalyzed reaction of **4a** with excess pyrrole, with the latter used as a solvent, was used to produce the bispyrrolylphenyl intermediate **6** in 68% yield after chromatographic purification (silica gel, EtOAc/hexanes 1:3 v/v, eluent). In contrast to analogous tripyrranes[40, 41] compound **6** proved quite stable, even in the presence of light and moisture. Unfortunately, the condensation between pyrrole **5**, acetone, and **6** in acetonitrile at room temperature in the presence of $BF_3 \cdot Et_2O$ provided compound **2a** in a maximum yield of 20%. Given this, the direct condensation approach shown in Scheme 2 remains the currently favored entry into systems of this type.

While an initial communication from our group described the general synthesis of chlorine-substituted calix[*n*]pyrrole[*m*]pyridine systems ($n + m = 4$), efforts to isolate cleanly the specific calix[3]pyrrole[1]pyridine species **7** analogous to the mixed phenyl/pyrrole/pyridine hybrid **3** were not successful at the time.[39] This important "control" compound has now been prepared in 45% yield from calix[4]pyrrole **8** as shown in Scheme 3.

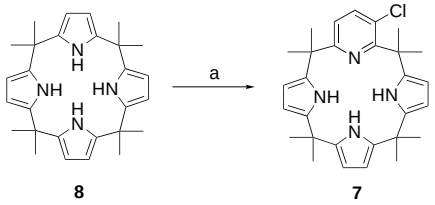

Scheme 3. Synthesis of calix[1]pyridine[3]pyrrole **7**. a) dimethoxyethane, sodium trichloroacetate (45%).

The availability of the "matched set" of hybrid compounds **1**–**3** and control compounds **7** and **8** allow a number of important structural and chemical comparisons to be made. To date, solid-state X-ray diffraction analyses of new compounds **1a**, **1b**, **2b**, **3**, and **7** have been carried out. In the case of **1a**, such analyses served to confirm not only the proposed

  0947-6539/02/0805-1135 $ 17.50+.50/0

structure, including the *trans*-like conformation of the two phenyl moieties (c.f. Figure 1), but also the ability of this species to interact with dimethoxyethane and dichloromethane in the solid state (Figures 2 and 3). In the case of the solvent-free structure, the individual phenyl and pyrrole rings are oriented in a 1,3-alternate-type conformation. Specifically, the protons on the 2-position of the benzene subunits ("2-position protons") are seen to point in opposite directions than the NH protons at the "center" of the pyrrolic rings. The resulting structure thus bears direct analogy to what is seen in the case of calix[4]pyrrole **8** in the absence of a bound substrate.[4] The rim-to-rim distances between the 2-position protons on the benzene subunits (D_1) and the two sets of 5-position protons on the benzene subunits (D_2) are 3.47 and 9.87 Å, respectively, making the angle of the vaselike structure approximately 125° relative to a pure cylinder-like species, wherein these two key protons would be oriented directly above one another (c.f. Figure 4). Other relevant structural parameters for this and the other structures are included in the figure captions.

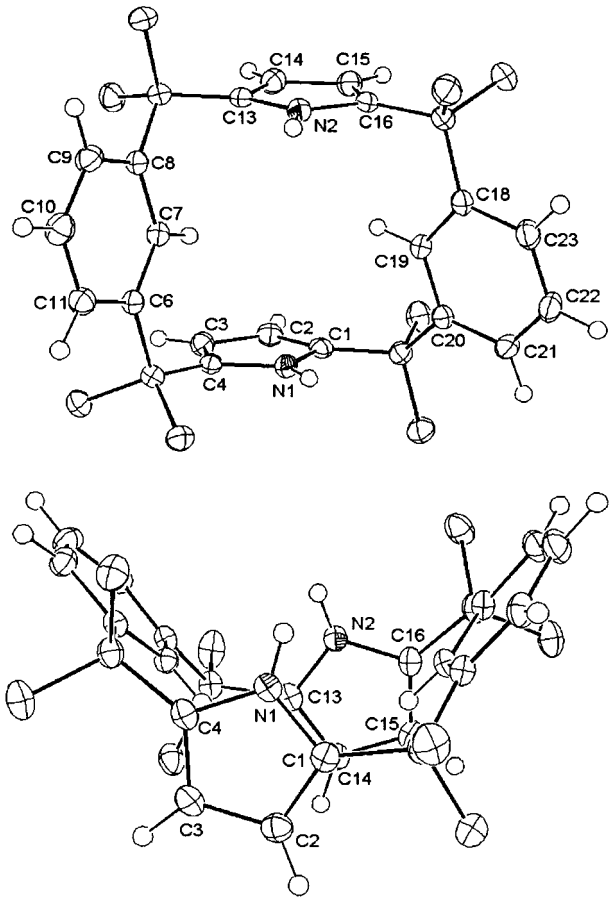

Figure 1. Two ORTEP views of **1a** showing the molecule as seen from the top with the atom labeling scheme partially indicated (top) and the molecule viewed from the side (bottom). Thermal ellipsoids are scaled to the 50% probability level. Hydrogen atoms are drawn to an arbitrary size. Methyl hydrogen atoms have been removed for clarity.

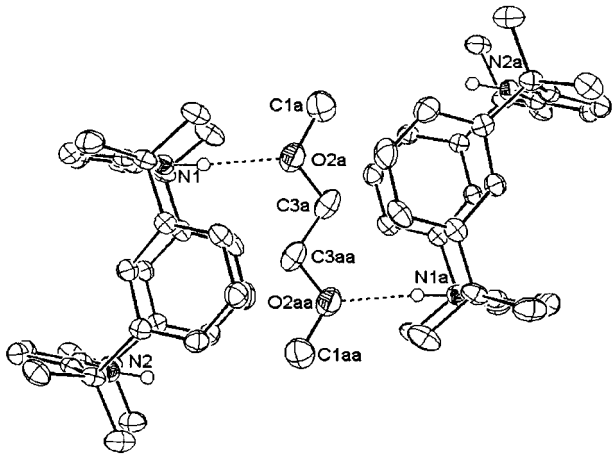

Figure 2. ORTEP view of the hydrogen bond dimer formed in **1a** showing a partial atom labeling scheme. Displacement ellipsoids are scaled to the 50% probability level. Most hydrogen atoms have been removed for clarity. The dimer lies around a crystallographic inversion center at 1/2, 1/2, 1/2. Dashed lines are indicative of the hydrogen-bonding interactions. The geometry of these interactions is: N1–H1N···O2a, N···O 3.041(2) Å, H···O 2.11(2) Å, N–H···O 175(2)°.

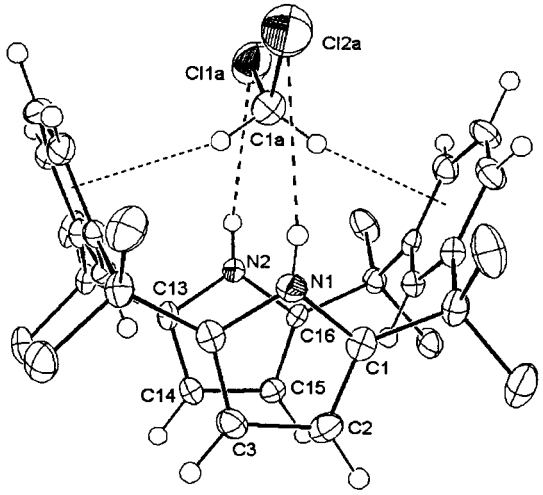

Figure 3. ORTEP view of **1a**·CH_2Cl_2 showing the hydrogen bonding interactions between the solvent and the macrocycle. Thermal ellipsoids are scaled to the 50% probability level. Dashed lines are indicative of hydrogen-bonding interactions. The geometry of these interactions are: N1–H1N···Cl2a: N···Cl 4.093(3) Å, H···Cl 3.38(3) Å, N–H···Cl 152(3)°; N2–H2N···Cl1a: N···Cl 3.680(3) Å, H···Cl 2.87(3) Å, N–H···Cl 163(3)°; C1a–H1ab—ring center of atoms C6, C7, C8, C9, C10, and C11: C···ring center 3.418(4) Å, H···ring center 2.45 Å, C–H···ring center 168°; C1a–H1aa—ring center of atoms C18, C19, C20, C21, C22, and C23: C···ring center 3.395(4) Å, H···ring center 2.49 Å, C–H···ring center 164°.

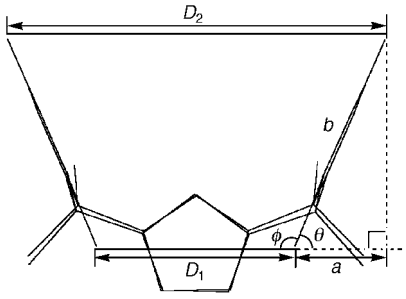

Figure 4. Schematic representation of the vaselike structure of **1a** showing relevant summary distance and angle parameters. D_1 and D_2 were obtained from the X-ray diffraction analysis and are 3.47 and 9.87 Å, respectively. Distance *a* was calculated as 3.2 Å = (9.87 – 3.47)/2, whereas distance *b* was taken as the distance between the protons on the *para* position of the benzene subunits (4.96 Å). These calculations lead to angles ϕ and θ being 125° and 55°, respectively.

0947-6539/02/0805-1136 $ 17.50+.50/0 *Chem. Eur. J.* **2002**, *8*, No. 5

In the presence of dimethoxyethane, a complex structure is seen wherein two calix[2]benzene[2]pyrrole macrocycles **1a** form a sandwich-like capsule around the solvent guest (Figure 2). Here, specific hydrogen-bonding interactions between the pyrrole NH and the ether oxygen atoms are believed to play a stabilizing role. This structure thus differs from what is seen in the case of dichloromethane. In this instance, a 1:1 structure is observed in the solid state, with both NH···Cl and CH_2Cl_2···phenyl-face hydrogen-bonding interactions appearing to play a stabilizing role (c.f. Figure 3). In this case, as is true in the case of the dimethoxyethane structure of Figure 2, the macrocycle remains in a 1,3-alternate conformation. While not necessarily predictable, a priori, the fact that this conformation is retained in the presence of the bound dimethoxyethane substrate is not altogether surprising, since, in contrast to what is true for calix[4]pyrrole **8**, hybrid **1a** does not contain four aryl subunits (viz. pyrroles) that can participate readily in hydrogen bonding. The driving force to adopt a cone conformation in the presence of a substrate is thus reduced.[42]

The *trans*-calix[2]-5-methoxybenzene[2]pyrrole **1b** differs from **1a** in that it contains "built-in" methoxy groups. As such, it contains both hydrogen-bond donors and acceptors within its framework. Presumably as a consequence of this duality, it exists as an offset dimer in the solid state. Here, as illustrated in Figure 5, the two individual macrocyclic subunits are linked through two hydrogen-bonding interactions that involve collectively the 5-methoxybenzene oxygen atoms and the pyrrole NH protons.

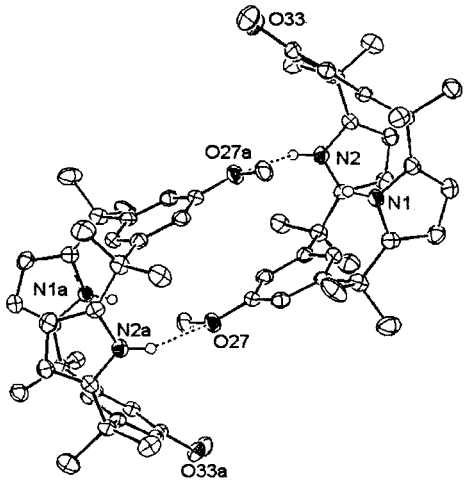

Figure 5. ORTEP view of the hydrogen-bound dimer formed by **1b**. Displacement ellipsoids are scaled to the 50% probability level. Most hydrogen atoms have been removed for clarity. The dimer lies around a crystallographic inversion center at 1/2, 1/2, 0. The geometry of the hydrogen-bonding interaction is: N2–H2N···O27 (related by $1-x$, $1-y$, $-z$): N···O 3.319(3) Å, H···O 2.54(2) Å, N-H···O 146(1)°.

Calix[1]-5-methoxybenzene[3]pyrrole **2b**, an analogue of **1b** with a single methoxy substitutent, is also found to exist as a dimer in the solid state, as revealed by X-ray diffraction analysis. As in **1b**, two hydrogen bonds involving the methoxy oxygen atoms of the 5-methoxybenzenes and the NH protons of the flanking pyrroles are involved in stabilizing the dimeric structure. On the other hand, the dimer is far from symmetric with the two relevant H···O distances, 2.08 and 2.55 Å, being far from equal. Overall, each of the macrocyclic subunits in the dimer is best characterized as being in the 1,3-alternate conformation (Figure 6).

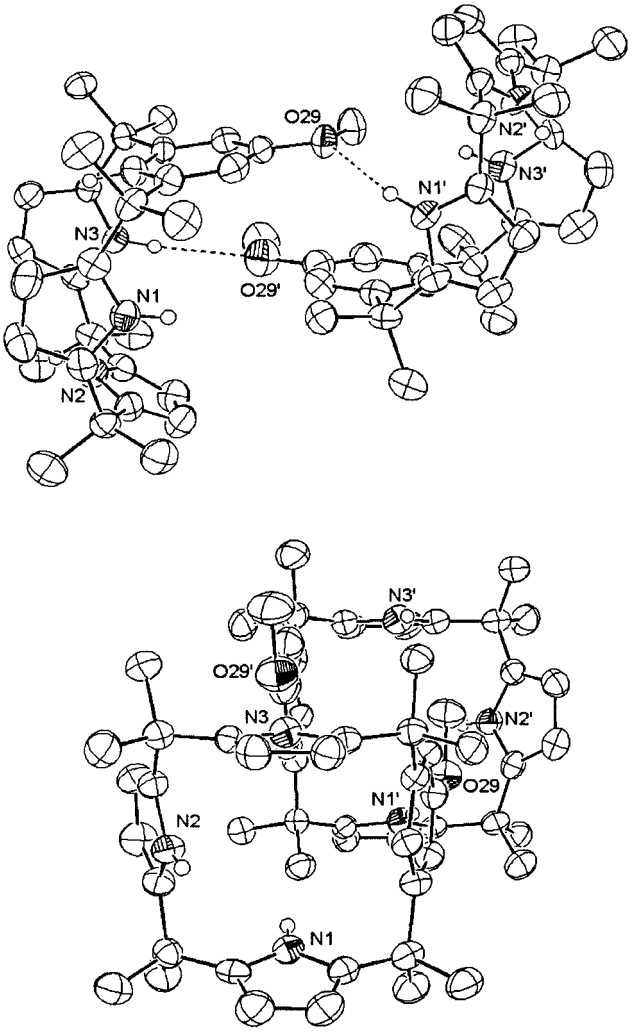

Figure 6. Two ORTEP views of the hydrogen-bound dimer formed in **2b** showing the molecule viewed from the top with a partial atom labeling scheme (top) and the molecule viewed from the side (bottom). Displacement ellipsoids are scaled to the 30% probability level. Most hydrogen atoms have been removed for clarity. The H-bonding interaction is not symmetrical between the two molecules. The N1′···O29 contact (2.960(5) Å) is closer than that found for N3···O29′ contact (3.428(5) Å). The complete geometry of this interaction is: N1′–H1′N···O29: N···O 2.960(5) Å, H···O 2.08 Å, N–H···O 166°; N3–H3N···O29′: N···O 3.428(5) Å, H···O 2.55 Å, N–H···O 165°.

The X-ray structure of compound **3** is shown in Figure 7. Not surprisingly, this macrocycle, containing as it does three different aromatic subunits (i.e., pyrrole, pyridine, and benzene), exhibits more distortion than its congeners containing only two kinds of building blocks. In particular, the benzene ring between the chloropyridine and the pyrrole subunits is "flattened out", while the pyridine and pyrrole rings are twisted away from each other. On the other hand, the system as a whole shows elements in common with a more

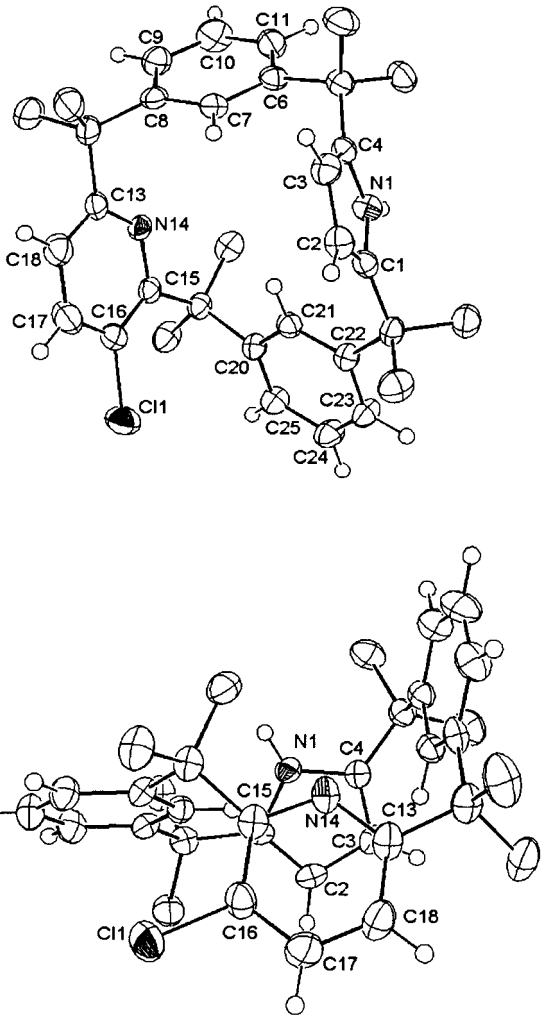

Figure 7. Two ORTEP views of **3** showing its flattened partial cone structure. Top: the molecule viewed from the top with the atom labeling scheme; bottom: the molecule as seen from the side. Displacement ellipsoids are scaled to the 50% probability level. Most hydrogen atoms have been removed for clarity. The geometry of the bond angles are: N1–C1–C26 121.3(2)°, N1–C4–C5 121.5(2)°, N14–C13–C12 115.9(2)°, N14–C15–C19 116.1(2)°.

classic 1,3-alternate conformation. The net result is an overall structure that is maybe best described as "flattened partial cone". Interestingly, although the crystals used to solve this particular structure were grown from a mixture of dichloromethane and ethanol, no interactions with solvent are seen; neither are interactions between individual calix[2]benzene[1]pyridine[1]pyrrole molecules observed. The system thus remains rigorously monomeric, at least in the solid state.

Flattened partial-cone solid-state conformations are also seen in the case of **7**. Here, two separate X-ray structures were solved. The first set of crystals were grown from dichloromethane/hexanes and in this instance, X-ray diffraction analysis revealed the presence of dimers. As shown in Figure 8, these dimers are linked by pyrrole-to-chloropyridine (NH···Cl) hydrogen-bonding interactions. When crystals of this same compound were grown in the presence of methanol, an infinite chain, rather than discrete dimer-like arrangement was seen in the solid state (Figure 9). The chains themselves

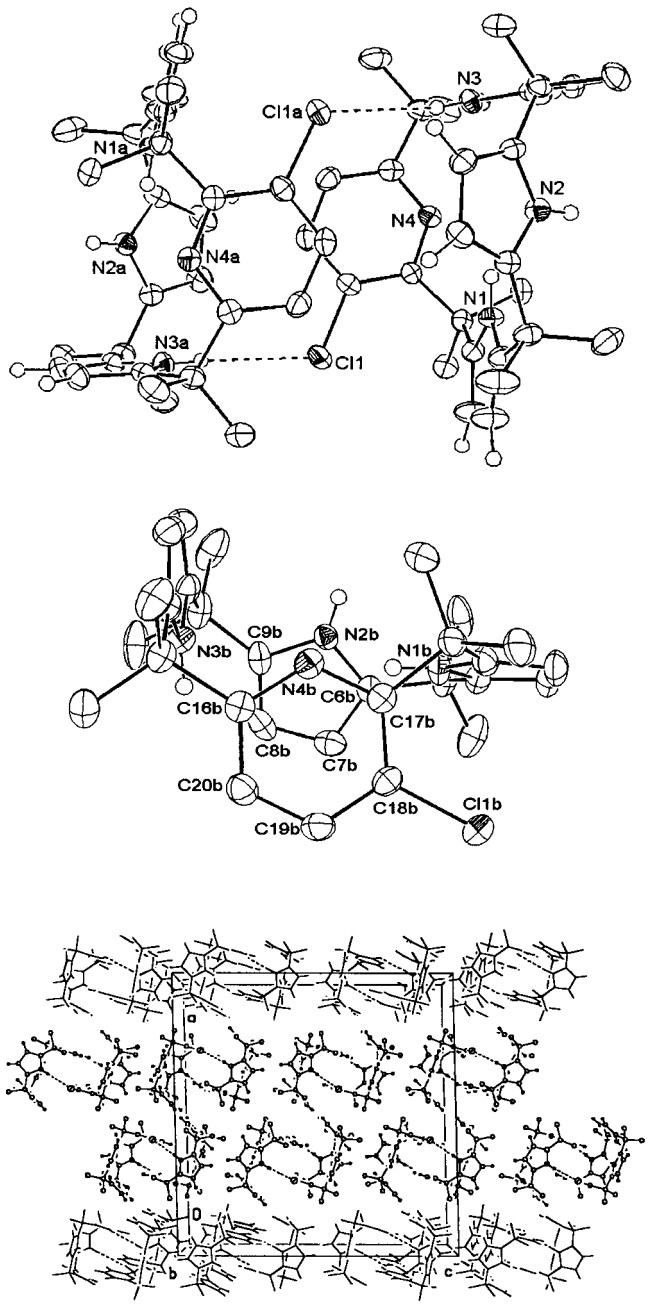

Figure 8. Top: ORTEP view of the hydrogen-bound dimer formed by **7**. Middle: Side view an isolated molecule of **7** illustrating the flattened partial cone structure it adopts in the solid state. Displacement ellipsoids are scaled to the 30% probability level. Most hydrogen atoms have been removed for clarity. The geometry of the hydrogen-bonding interactions are: N3–H3N···Cl1A: N···Cl 3.482(2) Å, H···Cl 2.67(2) Å, N–H···Cl 172(2)°; N3A–H3NA···Cl1: N···Cl 3.483(2) Å, H···Cl 2.65(2) Å, N–H···Cl 175(2)°. Bottom: Fragment of the infinite structure found in crystals of **7** highlighting the fact that three separate molecules are seen in the solid state, all with similar structure parameters. Molecules 1 and 2 form hydrogen-bound dimers around noncrystallographic, approximate inversion centers at 0.67, 0.36, 0.09. Molecules of type 3 form columns of hydrogen-bound molecules. These columns extend parallel to the *b* axis.

are set up, and presumably stabilized, by both pyrrole-to-methanol (NH···O) and pyrrole-to-chloropyridine (NH···O) hydrogen-bonding interactions.

The ^{1}H and ^{13}C NMR spectra of compounds **1**–**3** and **7** proved consistent with the proposed structures and config-

0947-6539/02/0805-1138 $ 17.50+.50/0 *Chem. Eur. J.* **2002**, *8*, No. 5

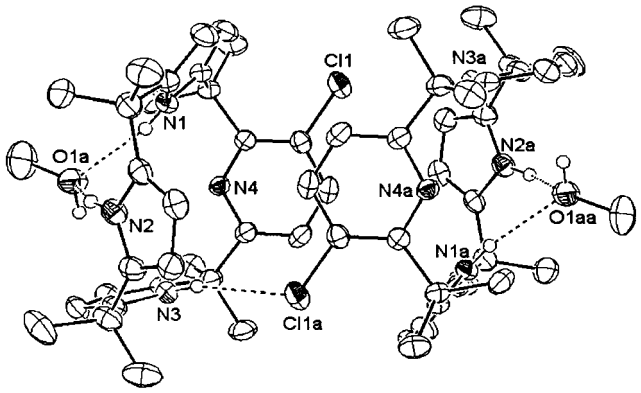

Figure 9. ORTEP view of the hydrogen-bound dimer formed by **7** in methanol showing a partial atom labeling scheme. Displacement ellipsoids are scaled to the 30% probability level. Most hydrogen atoms have been removed for clarity. The dimer lies around a crystallographic inversion center at 1/2, 0, 0. Dashed lines are indicative of hydrogen-bond interactions. The chlorine atom of one molecule is hydrogen bound to a pyrrole group on an adjacent molecule. The geometry of this interaction is: N3–H3N···Cl1 (related by $1-x$, $-y$, $-z$): N···Cl 3.482(1) Å, H···Cl 2.66(2) Å, N–H···O 165(2)°.

urations (c.f. Experimental Section). On the other hand, detailed analyses of the ^{1}H NMR spectra of compounds **1a**, **2a**, **3**, and **7** carried out in CD_2Cl_2, revealed that these prototypic species, while best described as being in conformations analogous to those seen in the solid sate, are nonetheless subject to dynamic distortions. As in the case of calix[4]pyrrole,[43–45] these motions are rapid at room temperature and begin to slow on the NMR timescale only at 188 K. While detailed analyses of the conformations present at room temperature are ongoing, they are believed to involve principally breathing motions such as those illustrated in Scheme 4, although rapid interconversions between the dominant 1,3-alternate and flattened partial-cone conformations highlighted in these schemes (and seen in the solid state) and more minor species (e.g., cone) cannot be rigorously ruled out.

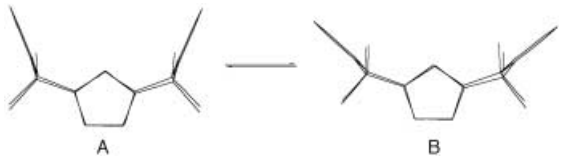

Scheme 4. Dominant conformations of **1a** believed to exist in rapid equilibrium at room temperature. Lowering the temperature to 188 K serves to stabilize the conformation shown on the right (structure B).

At low temperature (188 K; CD_2Cl_2), where the conformational motions were reduced, the picture is clearer. Under these conditions, the ^{1}H NMR and NOESY spectra of **1a**, **2a**, **3**, and **7** are consistent with the existence of only one conformer that closely resembles that seen in the solid state. For instance, in the case of **1a**, cross peaks between the 2-position benzene CH proton and both the β-pyrrolic protons and the NH protons are seen. By contrast, no cross peaks between the "outer" three benzene CH signals and the NH protons are observed. Neither are cross peaks seen between these outer benzene CH protons and β-pyrrole protons. Such observations rule out the significant presence of conelike conformations. On the other hand, they are fully consistent with a more flattened 1,3-alternate conformation such as illustrated by structure B in Scheme 4.

In the case of **2a**, cross peaks between the 2-position benzene CH and the NH and β-pyrrolic protons of the two flanking pyrroles are observed at 188 K. Cross peaks between the "central" pyrrole NH and the β-pyrrolic protons of the two flanking pyrroles are also observed. Again, the absence of cross peaks between the "outer" benzene CH and any β-pyrrolic protons, expected in the case of a cone conformation, is notable.

At low temperature (188 K; CD_2Cl_2), the less symmetric system **3** is characterized by a ^{1}H NMR spectrum with two separate "2-position" CH signals. One of these is seen to resonate at $\delta = 6.41$, while the other is found at $\delta = 5.58$. The upfield "shift" of the latter signal is consistent with it being positioned, in a relative sense, above one or more of the other aromatic subunits and, hence, within the influence of the associated ring current(s). The 2-position benzene CH signal at higher field is also seen to display cross peaks to the pyrrole NH in the NOESY spectrum. Conversely, the other 2-position benzene CH displays cross peaks with the β-pyrrolic and pyridine CH protons. This is consistent with the flattened partial-cone conformation seen in the solid.

Similar structural conclusions are drawn in the case of **7**. In this case, three separate pyrrole NH signals are observed at $\delta = 8.03$, 7.55, and 6.94, with one being shifted to higher field than the others. While the NOESY spectral analysis in this instance was complicated by the presence of overlapping signals, a clear set of cross peaks between the NH signal at lowest field ($\delta = 8.03$) and the pyridine CH and one set of the three independent β-pyrrolic CH signals was observed. Cross peaks between the NH signals at $\delta = 6.94$ and 7.55 could also be distinguished. Such interactions are expected in the case of a flattened partial-cone conformation, as is indeed seen in the solid state.

Compounds **1**–**3** and **7** contain fewer pyrrolic NH donor atoms than do the corresponding calix[4]pyrroles (e.g., **8**). They were thus expected to be weaker anion-binding agents. On the other hand, the observation that interactions with solvent and other hydrogen-bond acceptors were observed in the solid state, led us to explore the anion binding properties of **1a** and **2a**. Toward this end, standard proton NMR titration experiments were performed in CD_2Cl_2 at room temperature with tetrabutylammonium fluoride (TBAF) and tetrabutylammonium chloride (TBACl) as prototypical anionic substrates. In the case of **1a**, a system containing only two pyrrolic NH protons, the addition of 140 equivalents of TBAF to a solution of the macrocycle in CD_2Cl_2 at room temperature caused the pyrrolic NH signals to shift from $\delta = 6.67$ to $\delta =$ 8.25. On the other hand, these changes were nearly linear in concentration, with saturation in the degree of displacement not being reached at even the highest concentrations of added TBAF. As a result, it proved difficult to fit accurately the data to a standard 1:1 binding profile. To the extent such a fit could be made, it leads to the conclusion that macrocycle **1a** binds the fluoride anion with an affinity constant of $\leq 10\,\mathrm{M}^{-1}$ in CD_2Cl_2.

In contrast to **1a**, macrocycle **2a**, contains three NH protons (two "flanking" and one "central"). It was thus expected to be a better anion-binding agent than its calix[2]benzene[2]pyrrole analogue **1a**. In this case, substantial *downfield* shifts were observed, not only for the NH signals as expected, but also for the 2-position CH proton of the benzene ring. This latter observation, involving a $\Delta\delta$ of 2 ppm upon the addition of 22 equiv of TBAF, leads us to propose that, in addition to the pyrrolic NH protons, this benzene CH atom is involved in fluoride anion binding in the case of **2a**. Consistent with this supposition, the affinity constants for fluoride and chloride anion binding, calculated using the shifts in the two different pyrrole NH protons signals and 2-position benzene CH signal, gave the same values within error, namely $570 \pm 70\,\text{M}^{-1}$ and $17 \pm 3\,\text{M}^{-1}$ for F^- and Cl^-, respectively. This point is illustrated in Figure 10, which show representative ^{1}H NMR titration curves and binding profiles. Further support for the proposed 1:1 stoichiometries came from Job plots.

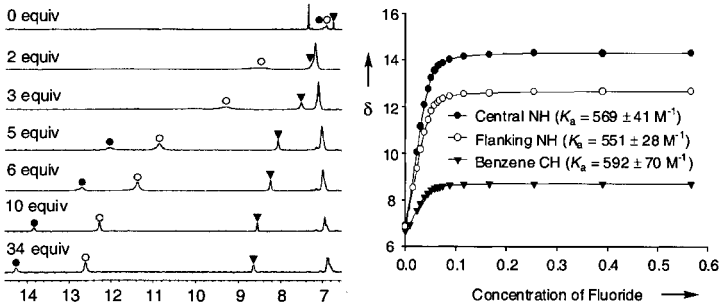

Figure 10. Left side: proton NMR spectral changes for the central NH (●), flanking NH (○), and central benzene CH (▼) protons observed upon the addition of TBAF to a CD_2Cl_2 solution of **2a**. Right side: observed and calculated 1:1 binding profiles associated with these shifts.

It is important to appreciate that the change in the 2-position benzene proton CH chemical shift seen in the case of **2a** is ascribed to anion binding and not to putative changes in conformation that could occur as the result of anion binding. For instance, an *upfield* shift of approximately 0.3 ppm is seen for the other ("outer") three benzene signals over the course of the titration of **2a** with TBAF. Likewise, an *upfield* shift of about 0.46 ppm is seen for the signal ascribed to the β-pyrrolic protons of the central pyrrole within the tripyrrane fragment, with an *upfield* shift of roughly 0.3 ppm being seen for the other two sets of β-pyrrolic signals. Such shifts are consistent with system **2a**, like calix[4]pyrrole **8** (Scheme 3), adopting a conelike conformation in the presence of a strongly bound anionic substrate (e.g., fluoride anion). Further support for this conclusion came from low-temperature NOESY analyses. For instance, cross peaks between the flanking pyrroles NH and both central pyrrole NH and the 2-position CH of benzene are seen in the low-temperature NOESY spectrum of **2a**·TBAF (188 K; CD_2Cl_2), signals that would not be seen were **2a** not in a cone conformation. Unfortunately, all efforts to obtain single crystals of **2a**·F^- suitable for X-ray diffraction analysis have so far met with failure.

Conclusion

In conclusion, we describe here synthetic strategies that have allowed for the construction of several novel heterocalixarenes containing two or three different heterocyclic building blocks. These "missing-link" macrocycles show structural features that are reminiscent of those seen in the case of calix[4]pyrroles, in particular a preference for 1,3-alternate or flattened partial-cone conformations in the solid state in the absence of strongly bound substrates, a high degree of flexibility at room temperature, and, in the case of the prototypic systems **1a** and **2a**, an ability to bind fluoride anion in solution, albeit less effectively than the "parent" calix[4]-pyrrole **8**, for which K_a values on the order of $17{,}000\,\text{M}^{-1}$ have been recorded in the same solvent system (CD_2Cl_2) used here.[4, 46] Current work is devoted to defining the conformational properties of these new heterocycles at room temperature more fully and to exploring further their substrate recognition properties. We are also seeking to quantify the relative importance of 2-position CH versus pyrrole NH hydrogen-bonding interactions as anion-binding motifs in artificial receptors.

Experimental Section

Dimethyl 5-methoxyisophthalate[47] was prepared according to the published procedure. Tetrabutylammonium fluoride trihydrate, purchased commercially, was dried under vacuum at 80 °C for 24 h prior to use in the binding studies. All other reagents were obtained from commercial sources and used as received. Proton NMR samples for use in the fluoride anion binding studies were prepared inside a Vacuum Atmospheres inert atmosphere glove box. The binding constant data were fit according to the method of Wilcox[48] by using changes in the NH. ^{1}H and ^{13}C NMR spectra used in the characterization of products were recorded on Varian Unity 300 MHz and Varian 500 MHz spectrometers. Low- and high-resolution mass spectra were obtained at the UT-Austin Department of Chemistry and Biochemistry MS Facility. Elemental analyses were performed by Atlantic Microlabs Inc., Norcross, GA.

***trans*-Calix[2]benzene[2]pyrrole (1a)**: Pyrrole (1 mL, 14.4 mmol) and 1,3-bis(1′,1′-dimethylhydroxymethyl)benzene (2.8 g, 14.4 mmol) were dissolved in acetonitrile (144 mL) at room temperature. The mixture was degassed with Ar for 5 min followed by the addition of $BF_3 \cdot Et_2O$ (1.8 mL, 14.4 mmol). The reaction mixture was stirred for 1 h, and quenched by the addition of 1N aqueous NaOH (ca. 10 mL). The mixture was extracted with EtOAc (3×150 mL) and the combined organic layers were washed with water and dried over Na_2SO_4. After removing the solvent by using a rotory evaporator, the resulting yellow solid was purified by column chromatography (silica gel; CH_2Cl_2/hexanes 1:2). Recrystallization from ethanol afforded **1a** in the form of a pure white solid (0.5 g, 16%). $R_f = 0.60$ (CH_2Cl_2/hexanes 1:1); m.p. 188 °C; ^{1}H NMR (300 MHz, $CDCl_3$, 25 °C): $\delta =$ 1.51 (s, 24H; *meso*-CH_3), 5.94 (d, ^3J (H,H) = 2.7 Hz, 4H; β-pyrrole CH), 6.59 (br s, 2H; NH), 6.74 (s, 2H; benzene CH^2), 7.19 (m, ^3J (H,H) = 1.2 Hz, 6H; benzene outer CH); ^{13}C NMR (75 MHz, $CDCl_3$, 25 °C): $\delta = 30.10$, 39.11, 103.17, 122.43, 126.60, 127.63, 139.41, 149.03; HRMS (CI +): calcd for $C_{32}H_{38}N_2$: 451.311325; found: 451.310716; elemental analysis calcd (%) for $C_{32}H_{38}N_2$ (450.3): C 85.28, H 8.50, N 6.22; found: C 85.18, H 8.54, N 6.24.

***trans*-Calix[2]-5-methoxybenzene[2]pyrrole (1b)**: By using a procedure analogous that used for the preparation of **1a**, pyrrole (155 μL, 2.2 mmol) and 1,3-bis(1′,1′-dimethylhydroxymethyl)-5-methoxybenzene (500 mg, 2.2 mmol) were reacted under Ar. The crude mixture was purified by column chromatography (silica gel, CH_2Cl_2/hexanes 1:1) and recrystallized from ethanol to afford **1b** in the form of a white solid (150 mg, 26%). $R_f =$ 0.46 (CH_2Cl_2/hexanes 2:1); m.p. 228 °C; ^{1}H NMR (300 MHz, $CDCl_3$, 25 °C): $\delta = 1.50$ (s, 24H; *meso*-CH_3), 3.78 (s, 6H; OCH_3), 5.93 (d, ^3J (H,H) = 2.7 Hz,

0947-6539/02/0805-1140 $ 17.50+.50/0 *Chem. Eur. J.* **2002**, *8*, No. 5

4H; β-pyrrole CH), 6.36 (t, ^3J (H,H) = 1.5 Hz, 2H; benzene CH^2), 6.60 (br s, 2H; NH), 6.73 (d, ^3J (H,H) = 1.5 Hz, 4H; benzene outer CH); ^{13}C NMR (75 MHz, $CDCl_3$, 25 °C): δ = 30.00, 39.15, 55.12, 102.91, 108.30, 119.23, 139.46, 150.45, 159.04; HRMS (CI+): calcd for $C_{34}H_{42}N_2O_2$: 511.332454; found: 511.332556; elemental analysis calcd (%) for $C_{34}H_{42}N_2O_2 \cdot H_2O$ (528.3): C 77.24, H, 8.39, N, 5.30; found: C 77.61, H 7.99, N 5.29.

Calix[1]benzene[3]pyrrole (2a)

Method A: A mixture of 1,3-bis-[1′-(pyrrol-2-yl)-1′,1′-(dimethyl)methyl]-benzene (1 g, 3.4 mmol), pyrrole (238 μL, 3.4 mmol), and acetone (510 μL, 7.0 mmol) in acetonitrile (170 mL) was degassed with Ar at room temperature for 5 min, and $BF_3 \cdot Et_2O$ (434 μL, 3.4 mmol) was added. The solution was stirred for 1 h under Ar and then quenched by the addition of 1N aqueous NaOH (ca. 1 mL). The aqueous mixture was extracted with EtOAc (3 × 200 mL), and the combined organic layers were washed with water several times. The solution was dried over Na_2SO_4 and filtered. After removing the solvent on the rotory evaporator, the resulting yellow solid was purified by column chromatography (CH_2Cl_2/hexanes 2:1). Recrystallization from ethanol afforded **2a** in the form of a pure white solid (0.3 g, 20%).

Method B: $BF_3 \cdot Et_2O$ (456 μL, 3.6 mmol) at room temperature under Ar was added to a mixture of pyrrole (1 mL, 14.4 mmol) and 1,3-bis(1′,1′-dimethylhydroxymethyl)benzene (0.7 g, 3.6 mmol) in acetonitrile (70 mL). The solution was stirred for 5 min at room temperature, and freshly distilled acetone (530 μL, 7.2 mmol) was added. The reaction mixture was stirred for an additional 55 min at room temperature. The reaction was quenched by the addition of about 1 mL triethylamine and diluted with water. The aqueous mixture was extracted with EtOAc (3 × 100 mL), and the combined organic layers were dried over Na_2SO_4 and filtered. After removing the volatile components on a rotory evaporator, the resulting residue was purified by column chromatography (silica gel, CH_2Cl_2/hexanes 2:1). Recrystallization from ethanol afforded **2a** in the form of a pure white solid (0.3 g, 18%). R_f = 0.70 (CH_2Cl_2/hexanes 3:1); m.p. 236 °C; ^{1}H NMR (300 MHz, $CDCl_3$, 25 °C): δ = 1.47 (s, 12H; *meso*-CH_3), 1.51 (s, 12H; *meso*-CH_3), 5.79 (d, ^3J (H,H) = 2.7 Hz, 2H; central β-pyrrole CH), 5.91–5.96 (m, 4H; flanking β-pyrrole CH), 6.68 (s, 1H; benzene CH^2), 6.82 (br s, 2H; NH), 6.96 (br s, 1H; NH), 7.27 (d, ^3J (H,H) = 1.2 Hz, 3H; benzene outer CH); ^{13}C NMR (75 MHz, $CDCl_3$, 25 °C): δ = 29.04, 30.32, 35.12, 39.14, 101.92, 103.09, 103.36, 122.53, 127.12, 127.83, 137.47, 138.53, 140.15, 148.73; HRMS (CI+): calcd for $C_{30}H_{37}N_3$: 440.306574; found: 440.305824; elemental analysis calcd (%) for $C_{30}H_{37}N_3$ (439.3): C 81.96, H 8.48, N 9.56; found: C 81.70, H 8.42, N 9.56.

Calix[1]-5-methoxybenzene[3]pyrrole (2b): Following the procedure of Method B above, pyrrole (1.2 mL, 17.3 mmol), and 1,3-bis(1′,1′-dimethyl-hydroxymethyl)-5-methoxybenzene (1 g, 4.5 mmol) were reacted under Ar. The crude mixture was purified by column chromatography (silica gel, CH_2Cl_2/hexanes 2:1) and recrystallized from ethanol giving **2b** in the form of a white solid (0.3 g, 13%). R_f = 0.50 (CH_2Cl_2/hexanes 2:1); m.p. 236 °C; ^{1}H NMR (300 MHz, $CDCl_3$, 25 °C): δ = 1.47 (s, 12H; *meso*-CH_3), 1.50 (s, 12H; *meso*-CH_3), 3.84 (s, 3H; OCH_3), 5.80 (d, ^3J (H,H) = 2.7 Hz, 2H; central β-pyrrole CH), 5.90–5.94 (m, 4H; flanking β-pyrrole CH), 6.26–6.27 (s, 1H; benzene CH^2), 6.80 (d, ^3J (H,H) = 1.8 Hz, 2H; benzene outer CH), 6.82 (br s, 2H; NH), 6.93 (br s, 1H; NH); ^{13}C NMR (75 MHz, $CDCl_3$, 25 °C): δ = 29.05, 30.24, 35.13, 39.22, 55.24, 101.97, 103.07, 103.28, 108.35, 119.76, 137.48, 138.53, 140.05, 150.26, 159.13; HRMS (CI+): calcd for $C_{31}H_{39}N_3O$: 470.317138; found: 470.316544; elemental analysis calcd (%) for $C_{31}H_{39}N_3O$ (469.3): C 79.28, H 8.37, N 8.95; found: C 79.02, H 8.29 , N 8.79.

***trans*-Calix[2]benzene[1]-3-chloropyridine[1]pyrrole (3)**: Sodium trichloroacetate (2.5 g, 13.5 mmol) was added to a solution of **1a** (1 g, 2.2 mmol) in dimethoxyethane (125 mL) at room temperature. The reaction mixture was heated at reflux for 6 h under Ar. After cooling to room temperature, hexanes (50 mL) were added. The reaction mixture was filtered through Celite and silica gel with dichloromethane as a washing solvent. Following removal of the volatile components on a rotory evaporator, the crude mixture was purified by column chromatography (silica gel, hexanes/CH_2Cl_2 3:2). Subsequent recrystallization from ethanol gave **3** in the form of a white solid (0.4 g, 36%). R_f = 0.56; m.p. 180 °C; ^{1}H NMR (300 MHz, $CDCl_3$, 25 °C, TMS): δ = 1.50 (s, 6H; *meso*-CH_3), 1.53–1.56 (m, 12H; *meso*-CH_3), 1.71 (s, 6H; *meso*-CH_3), 5.69–5.76 (m, 2H; β-pyrrole CH), 5.82 (s, 1H; benzene CH^2), 6.48 (s, 1H; benzene CH^2), 7.10 (d, ^3J (H,H) = 8.1 Hz, 1H; pyridine CH), 7.21–7.32 (m, 5H; benzene outer CH), 7.36–7.41 (m, 3H; pyridine CH and NH); ^{13}C NMR (75 MHz, $CDCl_3$, 25 °C): δ = 29.18, 29.92, 30.45, 39.01, 39.67, 45.34, 46.91, 104.63, 104.72, 119.07, 121.11, 122.03, 125.39, 127.28, 127.57, 127.81, 128.30, 137.60, 138.18, 148.74, 149.29, 150.22, 150.37, 160.80, 164.12; HRMS (CI−): calcd for $C_{33}H_{37}ClN_2$: 496.264527; found: 496.263735; elemental analysis calcd (%) for $C_{33}H_{37}ClN_2$ (496.3): C 79.73, H 7.50, N 5.64; found: C 79.57, H 7.39, N 5.52.

1,3-Bis-[1′-(pyrrol-2-yl)-1′,1′-(dimethyl)methyl]benzene (6): A mixture of pyrrole (72 mL, 1.0 mol) and 1,3-bis(1′,1′-dimethylhydroxymethyl)benzene (10.1 g, 52.0 mmol) was degassed by bubbling with Ar gas for 5 min. Then, $BF_3 \cdot Et_2O$ (6.6 mL, 52.1 mmol) was slowly added to the reaction mixture. After the addition was complete, the reaction mixture was stirred for 20 min at room temperature, followed by dilution with CH_2Cl_2 (ca. 100 mL). The reaction mixture was quenched by the addition of 0.1N aqueous NaOH (ca. 10 mL), and the organic layer was washed with water several times until the pH of the washings was about 7. The organic layer was collected and dried over Na_2SO_4. After filtration and removal of the solvent on the rotory evaporator, brown oil was obtained that was purified by column chromatography (silica gel, EtOAc/hexanes 1:3). This afforded **6** in the form of a colorless oil (10.3 g, 68%). ^{1}H NMR (300 MHz, $CDCl_3$, 25 °C): δ = 1.62 (s, 12H; *meso*-CH_3), 6.07–6.13 (m, 4H; pyrrole CH), 6.62 (s, 2H; pyrrole CH), 7.00–7.03 (m, 2H; benzene CH), 7.15–7.19 (m, 2H; benzene CH), 7.63 (br s, 2H; NH); ^{13}C NMR (300 MHz, $CDCl_3$, 25 °C): δ = 30.02, 39.29, 104.31, 107.61, 116.60, 123.81, 124.08, 128.00, 140.32, 148.93; HRMS (CI+): calcd for $C_{20}H_{24}N_2$: 293.201774; found: 293.201032.

1,3-Bis(1′,1′-dimethylhydroxymethyl)-5-methoxybenzene (4b): The procedure reported by Hsu, Lucas, and Buchwald was modified as follows.[49] Dimethyl 5-methoxyisophthalate (6 g, 26.8 mmol) in toluene (100 mL) slowly over 5 min at room temperature to a mixture of methyl magnesium chloride (3.0M solution in THF, 40 mL, 120 mmol) and toluene (160 mL). The resulting mixture was heated at reflux for 2 h under Ar gas. After cooling, the reaction mixture was quenched with aqueous K_2CO_3 solution (20 mL). The aqueous mixture was extracted with EtOAc (3 × 100 mL), and the combined organic layers were washed with water several times. The organic layers were dried over Na_2SO_4 and filtered. Removal of the solvent gave a brown oil which was purified by column chromatography (silica gel, EtOAc/CH_2Cl_2 1:3) afford a colorless solid (5 g, 84%). M.p. = 110–112 °C; ^{1}H NMR (300 MHz, $CDCl_3$, 25 °C): δ = 1.57 (s, 12H; CH_3), 1.71 (br s, 2H; OH), 3.82 (s, 3H; OCH_3), 6.92 (d, ^3J (H,H) = 3.0 Hz, 2H; benzene CH), 7.17 (t, ^3J (H,H) = 1.7 Hz, 1H; benzene CH).

Calix[1]-3-chloropyridine[3]pyrrole (7): Following the general procedure given in reference,[41] calix[4]pyrrole **8** (0.43 mol, 0.99 mmol) and sodium trichloroacetate (0.56 g, 4.99 mmol) were reacted under Ar. The crude mixture was purified by column chromatography (silica gel, CH_2Cl_2/hexanes 1:1) giving **7** in the form of a brown solid (0.28 g, 45%). M.p. = 194 °C; ^{1}H NMR (300 MHz, $CDCl_3$, 25 °C): δ = 1.51 (s, 6H; *meso*-CH_3), 1.55 (s, 6H; *meso*-CH_3), 1.71–1.72 (m, 12H; *meso*-CH_3), 5.87–5.90 (m, 2H; β-pyrrole CH), 5.93–5.98 (m, 3H; β-pyrrole CH), 6.07–6.09 (m, 1H; β-pyrrole CH), 6.52 (br s, 1H; NH), 7.15 (d, ^3J (H,H) = 8.1 Hz, 1H; pyridine CH), 7.18 (br s, 1H; NH), 7.42 (d, ^3J (H,H) = 8.1 Hz, 1H; pyridine CH), 7.63 (br s, 1H; NH); ^{13}C NMR (300 MHz, $CDCl_3$, 25 °C): δ = 27.14, 27.82, 29.01, 29.66, 35.25, 35.61, 40.86, 42.70, 101.66, 102.24, 102.78, 104.05, 104.35, 105.01, 118.39, 128.42, 135.15, 137.05, 137.62, 138.56, 138.93, 139.12, 139.76, 159.09, 162.44; HRMS (CI+): calcd for $C_{29}H_{35}ClN_4$: 475.262850; found: 475.262443; elemental analysis calcd (%) for $C_{29}H_{35}ClN_4$ (474.3): C 73.32, H 7.43, N 11.79; found: C 73.19, H 7.38, N 11.62.

X-ray structure determinations: Crystal structure analyses were measured on a Nonius Kappa CCD diffractometer using a graphite monochromator with $Mo_{K\alpha}$ radiation (λ = 0.71073 Å). The data were collected at −120 °C by using an Oxford Cryostream low temperature device. Data reduction were performed with DENZO-SMN.[50] The structure was solved by direct methods with SIR92[51] and refined by full-matrix least-squares on F^2 with anisotropic displacement parameters for the non-H atoms by using SHELXL-97.[52] The hydrogen atoms were calculated in ideal positions with isotropic displacement parameters set to 1.2 × U_{eq} of the attached atom (1.5 × U_{eq} for methyl hydrogen atoms). The molecules crystallize as a hydrogen-bonded dimer through an N–H moiety of one of the pyrroles and the methoxy oxygen atom. The function, $\Sigma w(|F_o|^2 - |F_c|^2)^2$, was minimized, where $w = 1/[(\sigma(F_o))^2 + (0.045P)^2]$ and $P = (|F_o|^2 + 2|F_c|^2)/3$. $R_w(F^2) = [\Sigma w(|F_o|^2 - |F_c|^2)^2/\Sigma w(|F_o|)^4]^{1/2}$ where w is the weight given each reflection. $R(F) = \Sigma(|F_o| - |F_c|)/\Sigma|F_o|$ for reflections with $[F_o > 4\sigma(F_o)]$.

$S = [\Sigma w(|F_o|^2 - |F_c|^2)^2/(n-p)]^{1/2}$, where n is the number of reflections and p is the number of refined parameters. The data were corrected for secondary extinction effects. The correction takes the form: $F_{corr} = kF_c/[1 + (1.0(2) \times 10^{-6}) F_c^2 \lambda^3/(\sin 2\theta)]^{0.25}$, where k is the overall scale factor. Neutral atom scattering factors and values used to calculate the linear absorption coefficient are from the International Tables for X-ray Crystallography.[53]

Compound 1a: $C_{32}H_{38}N_2$; crystals grew as large colorless prisms by slow evaporation from EtOH/CH_2Cl_2. The data crystal was a prism of approximate dimensions $0.36 \times 0.35 \times 0.30$ mm; monoclinic, space group $C2/c$; $a = 24.6615(3)$, $b = 10.1842(1)$, $c = 20.7519(3)$ Å, $\alpha = \gamma = 90°$, $\beta = 93.711(1)°$, $V = 5201.07(11)$ Å^3, $Z = 8$, $\rho_{calcd} = 1.151$ g cm^{-3}, μ = none, $F(000) = 1952$; a total of 275 frames of data were collected by using ω scans with a scan range of 1.5° and a counting time of 216 s per frame. A total of 11185 reflections were measured, 5949 unique ($R_{int} = 0.0204$). The structure was refined on F^2 to 0.101, with $R(F)$ equal to 0.0422 and a goodness of fit, S, = 1.023.

Compound 1a · 1/2 $CH_3OCH_2CH_2OCH_3$: $C_{34}H_{43}N_2O$; crystals grew as large colorless prisms by slow evaporation from $C_4H_{10}O_2$. The data crystal was cut from a larger crystal and had approximate dimensions $0.36 \times 0.24 \times 0.16$ mm; triclinic, space group $P\bar{1}$, $a = 9.4918(2)$, $b = 10.3342(2)$, $c = 15.7844(4)$ Å, $\alpha = 84.714(1)°$, $\beta = 75.166(1)°$, $\gamma = 75.475(1)°$, $V = 1448.21(6)$ Å^3, $Z = 2$, $\rho_{calcd} = 1.137$ g cm^{-3}, $\mu = 0.068$ mm^{-1}, $F(000) = 538$; a total of 336 frames of data were collected by using ω scans with a scan range of 1° and a counting time of 41 s per frame. A total of 9317 reflections were measured, 6486 unique ($R_{int} = 0.0301$). The structure was refined on F^2 to 0.122, with $R(F)$ equal to 0.0535 and a goodness of fit, S, = 1.12.

Compound 1a · CH_2Cl_2: $C_{33}H_{40}N_2Cl_2$; crystals grew as colorless plates and lathes by slow evaporation from EtOH/CH_2Cl_2. The data crystal was a long lathe that had approximate dimensions $0.32 \times 0.25 \times 0.14$ mm; orthorhombic, space group $P2_12_12_1$, $a = 10.3893(2)$, $b = 15.1632(4)$, $c = 18.8540(5)$ Å, $\alpha = \beta = \gamma = 90°$, $V = 2970.17(12)$ Å^3, $Z = 4$, $\rho_{calcd} = 1.198$ g cm^{-3}, $\mu = 0.242$ mm^{-1}, $F(000) = 1144$; a total of 112 frames of data were collected by using ω scans with a scan range of 1.8° and a counting time of 423 s per frame. A total of 6125 reflections were measured, 6125 unique ($R_{int} = 0.0000$). The structure was refined on F^2 to 0.106, with $R(F)$ equal to 0.0696 and a goodness of fit, S, = 1.119.

Compound 1b: $C_{34}H_{42}N_2O_2$; colorless lathes and plates grown from EtOH/CH_2Cl_2. The data crystal was a plate that had approximate dimensions $0.33 \times 0.30 \times 0.22$ mm; triclinic, space group $P\bar{1}$, $a = 10.1811(2)$, $b = 10.5556(3)$, $c = 14.1719(4)$ Å, $\alpha = 97.219(1)°$, $\beta = 102.064(1)°$, $\gamma = 101.632(1)°$, $V = 1436.23(6)$ Å^3, $Z = 2$, $\rho_{calcd} = 1.181$ g cm^{-3}, $\mu = 0.073$ mm^{-1}, $F(000) = 552$; a total of 467 frames of data were collected by using ω scans with a scan range of 1° and a counting time of 43 s per frame. A total of 10316 reflections were measured, 6455 unique ($R_{int} = 0.0640$). The structure was refined on F^2 to 0.129, with $R(F)$ equal to 0.0550 and a goodness of fit, S, = 0.911.

Compound 2b: $C_{31}H_{39}N_3O$; crystals grew as colorless prism by slow evaporation from EtOH/CH_2Cl_2. The data crystal was cut from a larger crystal and had approximate dimensions $0.30 \times 0.29 \times 0.14$ mm; monoclinic, space group $P2_1/c$, $a = 10.2231(5)$, $b = 24.8417(9)$, $c = 21.4795(14)$ Å, $\alpha = \gamma = 90°$, $\beta = 92.521(3)°$, $V = 5449.6(5)$ Å^3, $Z = 8$, $\rho_{calcd} = 1.145$ g cm^{-3}, $\mu = 0.069$ mm^{-1}, $F(000) = 2032$; a total of 285 frames of data were collected by using ω scans with a scan range of 0.8° and a counting time of 185 s per frame. A total of 16390 reflections were measured, 8939 unique ($R_{int} = 0.1344$). The structure was refined on F^2 to 0.171, with $R(F)$ equal to 0.0768 and a goodness of fit, S, = 1.046.

Compound 3: $C_{33}H_{37}ClN_2$; crystals grew as colorless needles by slow evaporation from EtOH/CH_2Cl_2. The data crystal was cut from a long needle and had approximate dimensions $0.33 \times 0.08 \times 0.07$ mm; monoclinic, space group $P2_1/n$, $a = 10.0685(3)$, $b = 27.2258(8)$, $c = 10.4159(3)$ Å, $\alpha = \gamma = 90°$, $\beta = 107.202(2)°$, $V = 2727.52(14)$ Å^3, $Z = 4$, $\rho_{calcd} = 1.211$ g cm^{-3}, $\mu = 0.164$ mm^{-1}, $F(000) = 1064$; a total of 295 frames of data were collected by using ω scans with a scan range of 1° and a counting time of 231 s per frame. A total of 15811 reflections were measured, 6123 unique ($R_{int} = 0.1365$). The structure was refined on F^2 to 0.129, with $R(F)$ equal to 0.0599 and a goodness of fit, S, = 0.895.

Compound 7: $C_{29}H_{35}ClN_4$; crystals grew as large, colorless needles by slow evaporation from EtOH/hexanes. The data crystal was cut from a larger crystal and had approximate dimensions $0.40 \times 0.28 \times 0.20$ mm; monoclinic, space group $P2_1/c$, $a = 26.8813(2)$, $b = 10.8508(1)$, $c = 26.3360(3)$ Å, $\alpha = \gamma = 90°$, $\beta = 91.336(1)°$, $V = 7679.69(13)$ Å^3, $Z = 12$, $\rho_{calcd} = 1.233$ g cm^{-3}, $\mu = 0.174$ mm^{-1}, $F(000) = 304$; a total of 453 frames of data were collected by using ω scans with a scan range of 1° and a counting time of 120 s per frame. A total of 26713 reflections were measured, 17537 unique ($R_{int} = 0.0221$). The structure was refined on F^2 to 0.111, with $R(F)$ equal to 0.0586 and a goodness of fit, S, = 1.08.

Compound 7 · CH_3OH: $C_{30}H_{39}N_4OCl$; crystals grew as large, colorless prisms by slow evaporation from methanol. The data crystal was cut from a larger crystal and had approximate dimensions $0.40 \times 0.28 \times 0.20$ mm; monoclinic, space group $P2_1/n$, $a = 15.2157(2)$, $b = 10.2837(1)$, $c = 19.5280(3)$ Å, $\alpha = \gamma = 90°$, $\beta = 111.381(1)°$, $V = 2845.32(6)$ Å^3, $Z = 4$, $\rho_{calcd} = 1.184$ g cm^{-3}, $\mu = 0.163$ mm^{-1}, $F(000) = 1088$; a total of 292 frames of data were collected by using ω scans with a scan range of 1° and a counting time of 76 s per frame. A total of 10162 reflections were measured, 6487 unique ($R_{int} = 0.0218$). The structure was refined on F^2 to 0.109, with R(F) equal to 0.0453 and a goodness of fit, S, = 1.02.

CCDC-171491 (**1a**), CCDC-171489 (**1a** · 1/2 $CH_3OCH_2CH_2OCH_3$), CCDC-171492 (**1a** · CH_2Cl_2), CCDC-171493 (**1b**), CCDC-171494 (**2b**), CCDC-171490 (**3**), CCDC-171496 (**7**), and CCDC-171495 (**7** · CH_3OH.CCDC) contain the supplementary crystallographic data for this paper. These data can be obtained free of charge via www.ccdc.cam.ac.uk/conts/retrieving.html (or from the Cambridge Crystallographic Data Centre, 12 Union Road, Cambridge CB2 1EZ, UK; fax: (+44) 1223-336-033; or e-mail: deposit@ccdc.cam.ac.uk).

Acknowledgements

This work was supported by The National Institutes of Health (grant G.M. 58907 to J.L.S.) and the Ministry of Education of the Czech Republic (grant no. CEZ J19/98:223400008).

[1] P. D. Beer, J. B. Cooper in *Calixarenes in Action* (Eds.: L. Mandolini, R. Ungaro), Imperial College Press, London, **2000**, pp. 111 – 143.
[2] C. D. Gutsche, *Calixarenes Revisited*, The Royal Society of Chemistry, Cambridge, **1998**, pp. 23 – 27, pp. 146 – 208.
[3] G. J. Lumetta, R. D. Rogers, A. S. Gopalan, *Calixarenes for Seperations*, ACS, Washington, **2000**, pp. 107 – 312.
[4] P. A. Gale, J. L. Sessler, V. Král, *Chem. Commun.* **1998**, 1 – 8.
[5] S. Depraetere, M. Smet, W. Dehaen, *Angew. Chem.* **1999**, *111*, 3556 – 3558; Angew. *Chem. Int. Ed.* **1999**, *38*, 3359 – 3361.
[6] B. Turner, A. Shterenberg, M. Kapon, Y. Eichen, K. Suwinska, *Chem. Commun.* **2001**, 13 – 14.
[7] K. Ito, Y. Ohba, T. Tamura, T. Ogata, H. Watanabe, Y. Suzuki, T. Hara, Y. Morisawa, T. Sone, *Heterocycles* **1999**, *51*, 2807 – 2813.
[8] K. Ito, Y. Ohba, T. Tamura, T. Ogata, H. Watanabe, Y. Suzuki, T. Hara, Y. Morisawa, T. Sone, *J. Heterocycl. Chem.* **2001**, *38*, 293 – 298.
[9] Y.-S. Jang, H.-J. Kim, P.-H. Lee, C.-H. Lee, *Tetrahedron Lett.* **2000**, *41*, 2919 – 2923.
[10] B. Koenig, M. Roedel, P. Bubenitschek, P. G. Jones, *Angew. Chem.* **1995**, *107*, 752; *Angew. Chem. Int. Ed. Engl.* **1995**, *34*, 661 – 662.
[11] M. J. Marsella, K. Yoon, F. S. Tham, *Org. Lett.* **2001**, *3*, 2129 – 2131.
[12] D. S. C. Black, D. C. Craig, N. Kumar, *J. Chem. Soc. Chem. Commun.* **1989**, 425 – 426.
[13] D. S. C. Black, M. C. Bowyer, N. Kumar, P. S. R. Mitchell, *J. Chem. Soc. Chem. Commun.* **1993**, 819 – 821.
[14] D. S. Black, D. C. Craig, N. Kumar, *Tetrahedron Lett.* **1995**, *36*, 8075 – 8078.
[15] D. S. C. Black, D. C. Craig, N. Kumar, *Aust. J. Chem.* **1996**, *49*, 311 – 318.
[16] D. S. C. Black, D. B. McConnell, *Heteroat. Chem.* **1996**, *7*, 437 – 441.
[17] D. S. Black, N. Kumar, D. B. McConnell, *Tetrahedron* **2000**, *56*, 8513 – 8524.
[18] D. S. Black, N. Kumar, D. B. McConnell, *Tetrahedron* **2001**, *57*, 2203 – 2211.
[19] N. Kobayashi, S. Inagaki, V. N. Nemykin, T. Nonomura, *Angew. Chem.* **2001**, *113*, 2782 – 2784; *Angew. Chem. Int. Ed.* **2001**, *40*, 2710 – 2712.
[20] K. Agbaria, S. E. Biali, *J. Org. Chem.* **2001**, *66*, 5482 – 5489.
[21] N. Arumugam, Y.-S. Jang, C.-H. Lee, *Org. Lett.* **2000**, *2*, 3115 – 3117.

  0947-6539/02/0805-1142 $ 17.50+.50/0 *Chem. Eur. J.* **2002**, *8*, No. 5

[22] G. Cafeo, M. Giannetto, F. H. Kohnke, G. L. La Torre, M. F. Parisi, S. Menzer, A. J. P. White, D. J. Williams, *Chem. Eur. J.* **1999**, *5*, 356–368.
[23] G. Cafeo, F. H. Kohnke, G. L. La Torre, A. J. P. White, D. J. Williams, *Angew. Chem.* **2000**, *112*, 1556–1558; *Angew. Chem. Int. Ed.* **2000**, *39*, 1496–1498.
[24] R. M. Musau, A. Whiting, *J. Chem. Soc. Chem. Commun.* **1993**, 1029–1031.
[25] B. J. Shorthill, T. E. Glass, *Org. Lett.* **2001**, *3*, 577–579.
[26] M. Ashram, S. Mizyed, P. E. Georghiou, *J. Org. Chem.* **2001**, *66*, 1473–1479.
[27] A. Baeyer, *Ber. Dtsch. Chem. Ges.* **1886**, *19*, 2184–2185.
[28] W. E. Allen, P. A. Gale, C. T. Brown, V. M. Lynch, J. L. Sessler, *J. Am. Chem. Soc.* **1996**, *118*, 12471–12472.
[29] P. Anzenbacher, Jr., K. Jursikova, J. A. Shriver, H. Miyaji, V. M. Lynch, J. L. Sessler, P. A. Gale, *J. Org. Chem.* **2000**, *65*, 7641–7645.
[30] P. Anzenbacher, Jr., K. Jursikova, J. L. Sessler, *J. Am. Chem. Soc.* **2000**, *122*, 9350–9351.
[31] P. A. Gale, J. L. Sessler, J. W. Genge, V. Král, A. Andrievsky, V. Lynch, P. I. Sansom, W. E. Allen, A. Gebauer, C. T. Brown, *PCT Int. Appl.*, WO 9737995, **1997**, p. 145.
[32] J. L. Sessler, P. Anzenbacher, Jr., J. A. Shriver, K. Jursikova, V. M. Lynch, M. Marquez, *J. Am. Chem. Soc.* **2000**, *122*, 12061–12062.
[33] E. Weber, J. Trepte, V. C. Kravtsov, Y. A. Simonov, E. V. Ganin, J. Lipkowski, *J. Inclusion Phenom. Macrocyclic Chem.* **2000**, *36*, 247–257.
[34] E. Weber, J. Trepte, K. Gloe, M. Piel, M. Czugler, V. C. Kravtsov, Y. A. Simonov, J. Lipkowski, E. V. Ganin, *J. Chem. Soc. Perkin Trans. 2* **1996**, 2359–2366.
[35] J. Trepte, M. Czugler, K. Gloe, E. Weber, *Chem. Commun.* **1997**, 1461–1462.
[36] S. Kumar, G. Hundal, D. Paul, M. S. Hundal, H. Singh, *J. Org. Chem.* **1999**, *64*, 7717–7726.
[37] S. Kumar, D. Paul, H. Singh, *J. Inclusion Phenom. Macrocyclic Chem.* **2000**, *37*, 371–382.
[38] S. Kumar, G. Hundal, D. Paul, M. S. Hundal, H. Singh, *Perkin 1* **2000**, 2295–2301.
[39] V. Král, P. A. Gale, P. Anzenbacher, Jr., K. Jursikova, V. Lynch, J. L. Sessler, *Chem. Commun.* **1998**, 9–10.
[40] C. Bucher, D. Seidel, V. Lynch, V. Král, J. L. Sessler, *Org. Lett.* **2000**, *2*, 3103–3106.
[41] C. Bucher, R. S. Zimmerman, V. Lynch, V. Král, J. L. Sessler, *J. Am. Chem. Soc.* **2001**, *123*, 2099–2100.
[42] Even in the case of the calix[4]pyrroles, it is to be appreciated that non-cone conformations are seen in the case of complexes involving weak hydrogen bond acceptors (e.g., neutral solvents). See ref. [28].
[43] W. P. Van Hoorn, W. L. Jorgensen, *J. Org. Chem.* **1999**, *64*, 7439–7444.
[44] Y.-D. Wu, D.-F. Wang, J. L. Sessler, *J. Org. Chem.* **2001**, *66*, 3739–3746.
[45] D.-F. Wang, in *Abstracts of Papers, 222nd ACS National Meeting*, Chicago, IL (USA), August 26–30, **2001**, p. COMP-152.
[46] P. A. Gale, J. L. Sessler, V. Král, V. Lynch, *J. Am. Chem. Soc.* **1996**, *118*, 5140–5141.
[47] W. Dmowski, K. Piasecka-Maciejewska, *J. Fluorine Chem.* **1996**, *78*, 59–63.
[48] C. S. Wilcox in *Frontiers in Supramolecular OrganicChemistry and Photochemistry* (Eds.: H. -J. Schneider, H. Dürr), VCH, Weinheim, **1991**.
[49] D. P. Hsu, E. A. Lucas, S. L. Buchwald, *Tetrahedron Lett.* **1990**, *31*, 5563–5566.
[50] "Macromolecular Crystallography, Part A": *Methods Enzymol.* **1997**, *276*, whole issue.
[51] A. Altomare, G. Cascarano, C. Giacovazzo, A. Guagliardi, *J. Appl. Crystallogr.* **1993**, *26*, 343–350.
[52] G. M. Sheldrick, SHELX-97, Program for the refinement of Crystal Structures, University of Gottingen, Germany, **1994**.
[53] *International Tables for X-Ray Crystallography*, *Vol. C* (Eds.: J. S. Kasper, K. Lonsdale), Kluwer Academic Press, Boston, **1992**, Tables 4.2.6.8 and 6.1.1.4.

Received: October 1, 2001 [F3583]